Molecular Imaging

International Edition: DOI: 10.1002/anie.201509726
German Edition: DOI: 10.1002/ange.201509726

Catalytic Molecular Imaging of MicroRNA in Living Cells by DNA-Programmed Nanoparticle Disassembly

*Xuewen He, Tao Zeng, Zhi Li, Ganglin Wang, and Nan Ma**

Abstract: *Molecular imaging is an essential tool for disease diagnostics and treatment. Direct imaging of low-abundance nucleic acids in living cells remains challenging because of the relatively low sensitivity and insufficient signal-to-background ratio of conventional molecular imaging probes. Herein, we report a class of DNA-templated gold nanoparticle (GNP)–quantum dot (QD) assembly-based probes for catalytic imaging of cancer-related microRNAs (miRNA) in living cells with signal amplification capacity. We show that a single miRNA molecule could catalyze the disassembly of multiple QDs with the GNP through a DNA-programmed thermodynamically driven entropy gain process, yielding significantly amplified QD photoluminescence (PL) for miRNA imaging. By combining the robust PL of QDs with the catalytic amplification strategy, three orders of magnitude improvement in detection sensitivity is achieved in comparison with non-catalytic imaging probe, which enables facile and accurate differentiation between cancer cells and normal cells by miRNA imaging in living cells.*

MicroRNAs are a class of small, endogenous, non-coding RNA molecules that serve as critical regulators of gene expression.[1–3] Aberrant expression levels of miRNA are associated with a number of human diseases, including cancer, highlighting their potential as both diagnostic biomarkers and drug targets.[4–7] Direct imaging of miRNA in living cells would provide a valuable means for identifying cancerous cells and evaluating drug efficacy in real time. Conventional molecular beacons for nucleic acid sensing are designed on a one-to-one basis, where one target binds to and activates one probe for signal generation.[8–10] Although these probes are capable of detecting concentrated targets, they are not competent to accurately sense fluctuation of target quantity within low concentration ranges owing to relatively low sensitivity and insufficient signal-to-background ratio, limiting their usefulness for imaging low-abundance biomarkers. Sensitive optical imaging of nucleic acid molecules in living cells requires activatable probes with optimal responsivity to low target concentration and boosted signals to exceed the detection threshold of the microscope, which has not been fulfilled by traditional imaging probes. Although a variety of strategies based on enzymatic amplification have been established for high-sensitive analysis of miRNA in vitro and in fixed cells,[11–15] most of the these strategies are not suitable for direct imaging of miRNA in living cells.

Compared to conventional fluorophores, QDs have offered improved sensitivity for bioimaging owing to their strong and persistent photoluminescence (PL).[16–18] QDs could be bio-functionalized to specifically interact with a variety of biomolecular targets for bioimaging.[19–23] Despite these successes, it remains difficult to facilely distinguish QDs signal from the background if the targets are present at low concentration, which is prone to biased imaging results. The Willner and Ho groups recently report the use of QD probes for in vitro sensitive analysis of microRNAs.[14] QD-based probes with signal amplification capacity for sensitive in vivo imaging of low-abundance intracellular nucleic acids are highly desirable, yet remains undeveloped.

Herein, we developed a class of nanoparticle assembly-based imaging probe for high-sensitive catalytic imaging of miRNA in living cells. The probe comprises a GNP and several QDs tethered to the GNP surface through a DNA linker (Figure 1 a). PL of QDs is quenched by the nearby GNP through fluorescence resonance energy transfer (FRET). A single copy of miRNA target could trigger disassembly of multiple QDs with the GNP with the aid of fuel DNA strands, yielding significantly amplified imaging signals (Figure 1 a; Supporting Information, Scheme S1). Unlike traditional probes, the miRNA target serves as a catalyst to repeatedly unlock the DNA linkers to activate the probe and thus offers high detection sensitivity. As shown in Figure 1 a, GNPs (13 nm) and CdTe QDs (3.8 nm) are co-assembled on the linker strand (L) through DNA hybridization. DNA1-functionalized GNPs are prepared by attaching thiolated DNA to GNP surface (Figure S1).[24–26] DNA2-functionalized QDs are prepared using chimeric phosphorothioate-phosphate DNA molecules as templates to synthesize QDs (Figure S2).[23,27] The average numbers of DNA1 and linker DNA on each GNP are determined to be 37 and 23 respectively using a DTT displacement assay (Figure S3). DNA2-QDs contains 89 % monovalent QDs and 11 % bivalent QDs as revealed by native polyacrylamide gel electrophoresis (PAGE; Figure S4). Assembly of DNA1-GNPs and DNA2-QDs results in satellite nanostructures, as shown in the high-resolution transmission electron microscopy (HRTEM) image (Figure 1 b). There are 16 QDs on each GNP on average, as determined by elemental analysis. The GNP-QDs nanoassemblies are colloidal, stable under different ionic strength (0–1000 mM NaCl) and pH (4.0–10.0), and

[*] X. He, T. Zeng, Z. Li, G. Wang, Prof. N. Ma
State and Local Joint Engineering Laboratory for Novel Functional Polymeric Materials
The Key Lab of Health Chemistry and Molecular Diagnosis of Suzhou
College of Chemistry
Chemical Engineering and Materials Science, Soochow University
Suzhou, 215123 (P.R. China)
E-mail: nan.ma@suda.edu.cn

Supporting information, including experimental details, for this article is available on the WWW under http://dx.doi.org/10.1002/anie.201509726.

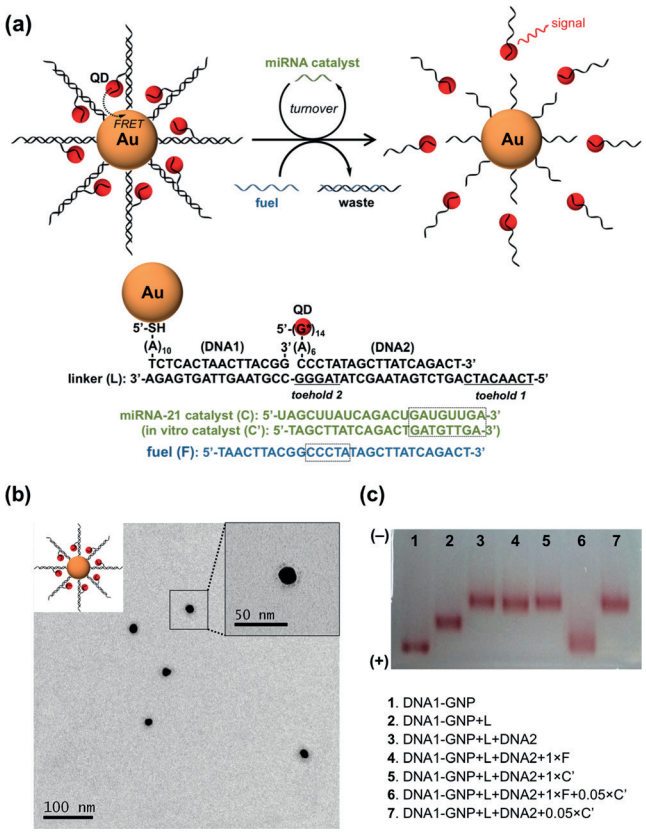

Figure 1. a) Illustration of GNP-QDs nanoassembly for catalytic miRNA sensing. The miRNA molecule serves as a catalyst to disassemble QDs from the GNP with the aid of fuel DNA strands. b) TEM images of GNP-QDs nanoassembly. c) Agarose gel electrophoresis for monitoring the catalytic disassembly reaction.

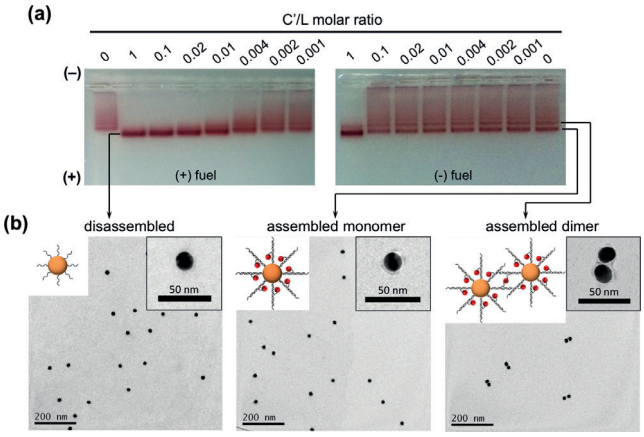

Figure 2. a) Agarose gel electrophoresis characterization of GNP-QDs disassembly under different C′/L molar ratios in the presence (left) and absence (right) of fuel DNA. b) TEM images of assembled GNP-QDs satellite monomer and dimer, and disassembled reaction products isolated from agarose gel.

remain intact in the presence of DNase I (50 U L^{-1}) or in the cell extract (Figure S5). The DNA linker is designed based on a thermodynamically driven entropy gain process,[28] where the fuel strand (F) displaces two short strands (DNA1 and DNA2) to form a free, double-stranded waste product. miRNA-21 is a common oncogenic miRNA that is upregulated in most kinds of cancers,[29,30] and was selected as an initial imaging target. The miRNA-21 strand (C) or the cognate DNA strand (C′) with the same sequence binds to toehold 1 (8 nt) and displaces DNA2 from the linker through branch migration to expose toehold 2 (5 nt); subsequently the fuel strand (F) binds to toehold 2 and liberates DNA1 and the catalyst strand (C/C′) (Scheme S1). To validate this design, we performed agarose gel electrophoresis to monitor the catalytic reaction. As shown in Figure 1c, successive assembly of DNA1-GNP with L and DNA2 resulted in retarded mobility of GNPs in the gel. Disassembly of GNP with L occurred in the presence of F (1×) and subtle amount of C′ (0.05×), but did not occur in the absence of C′, confirming that C′ could catalyze disassembly of GNPs with L.

We subsequently explored the dependence of GNP-QD catalytic disassembly on target concentration. As shown in Figure 2a, the unpurified GNP-QD nanostructure exhibited multiple discrete bands in the agarose gel. The two bands with highest mobility were isolated and observed under TEM. The lower major band corresponds to GNP-QD satellite monomers, and the upper minor band corresponds to GNP-QD satellite dimer consisting of a pair of GNPs (Figure 2b). The heterogeneity of the nanoassembly is expected because bivalent DNA2-QDs could crosslink GNPs to form higher-order nanostructures. Disassembly of GNP-QD nanostructure in the presence of F resulted in the disappearance of the higher-order nanostructure bands and a shift of the monomer band toward higher mobility, which could be visualized at a C′/L molar ratio of 0.04 and became more completed as the C′/L molar ratio increased (Figure 2a). TEM confirmed that the single band at C′/L molar ratio of 1 corresponds to the disassembled GNPs without QDs (Figure 2b). In contrast, disassembly of GNP-QD in the absence of F was observed only at a C′/L molar ratio of 1, but not at lower C′ L^{-1} molar ratios between 0.001 and 0.1 (Figure 2a), which suggests that stoichiometric target concentration is required to efficiently activate the probe by non-reversible target-probe binding. Disassembly of the GNP-QD nanostructure resulted in recovery of QD PL (Figures 3 and Figure S6). QD PL was enhanced by 3.5-, 8.8-, 20.1-, and 40.9-fold by catalytic disassembly at C′/L molar ratios of 0.001, 0.002, 0.004, and 0.01 respectively, revealing high responsivity of the GNP-QD nanoassembly to low target concentrations (Figure 3a and b). A near-linear relationship between the QD PL intensity and C′/L ratio was obtained at C′/L molar ratios between 0 and 0.01 (Figure 3c). In contrast, activation of QD PL in the absence of F was only detected at C′/L molar ratios above 0.2 (Figure 3b and d). The limit of detection (LOD) is calculated to be 4.56 pM for catalytic disassembly, which is about three orders of magnitude lower than non-catalytic disassembly (4.64 nM). Additionally, the GNP-QD probe would not be activated by non-target DNA with the sequence of miRNA-141 (Figure S7), indicating the selectivity of the detection system. The disassembly kinetics of GNP-QD nanostructure was characterized by measuring the QD PL intensities at different time points. As shown in Figure 3e, catalytic disassembly became faster with increasing reaction time or

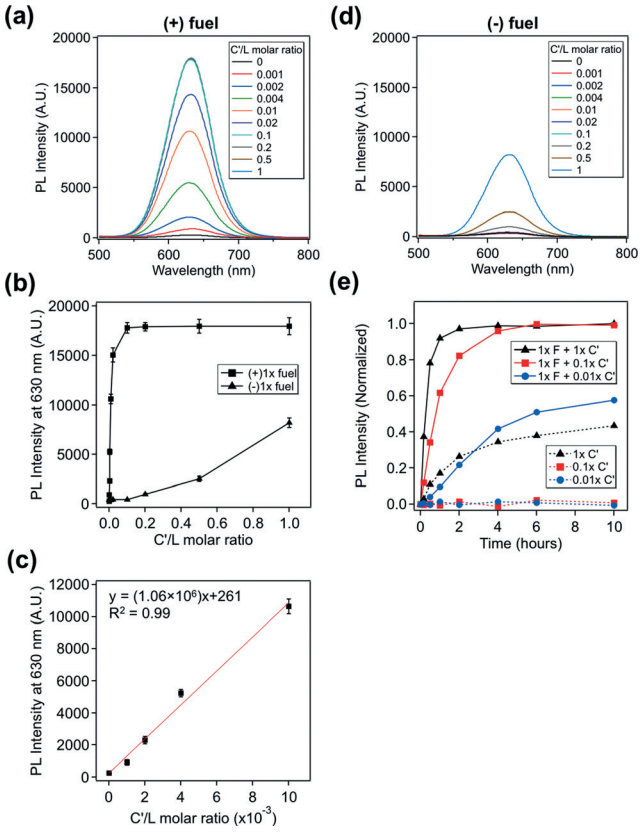

Figure 3. PL activation of GNP-QDs nanoassembly under different C′/L molar ratios. a) PL spectra of GNP-QDs nanoassembly under various C′/L molar ratios in the presence of fuel DNA. b) PL activation curves for catalytic and non-catalytic GNP-QDs disassembly as a function of C′/L molar ratio. c) Standard curve for quantitative analysis of miRNA target. d) PL spectra of GNP-QDs nanoassembly under various C′/L molar ratios in the absence of fuel DNA. e) GNP-QDs disassembly kinetics in the presence or absence of fuel DNA under various C′/L molar ratios.

target concentration. Efficient probe activation was achieved after 6 hours reaction at a C′/L molar ratio of 0.01, and this condition was selected for miRNA detection and imaging experiments. In contrast, the probe could not be activated in the absence of F at low C′/L molar ratios (0.01 and 0.1) even after prolonged incubation.

Next, we applied the GNP-QD nanoassembly for in vitro quantification of miRNA-21. Three cancer cell lines (HeLa, MCF-7, and MDA-MB-231) containing upregulated levels of miRNA-21, and a control cell line (HEK-293) with minimal level of miRNA-21, were examined. Total RNA extracted from each cell line was incubated with the GNP-QD nanoassembly and the QD PL was recorded. Pronounced recovery of QD PL was detected for total RNA extracted from HeLa, MCF-7, and MDA-MB-231 cells based on catalytic detection (Figure 4a and SI Figure S8). The miRNA-21 concentration in each total RNA sample was determined by converting the QD PL intensity to C/L molar ratio using the standard curve in Figure 3c. Copy numbers of miRNA-21 per pg of total RNA in HeLa, MCF-7, and MDA-MB-231 cells were calculated to be 323 ± 28, 746 ± 44, 706 ± 45, respectively

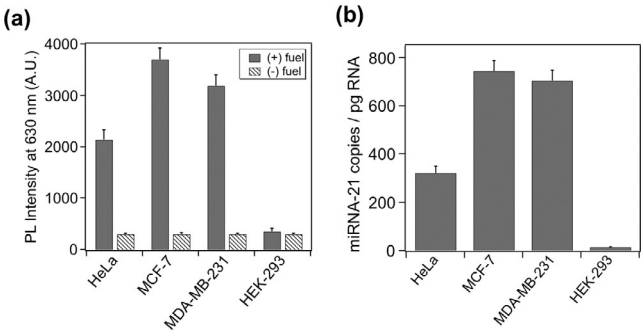

Figure 4. Quantitative analysis of miRNA-21 in total RNA extracted from HeLa, MCF-7, MDA-MB-231, and HEK-293 cells. a) PL intensity (630 nm) of GNP-QDs nanoassembly incubated with total RNA extracted from HeLa, MCF-7, MDA-MB-231, and HEK-293 cells in the presence or absence of fuel DNA. b) Copy numbers of miRNA-21 per pg total RNA from HeLa, MCF-7, MDA-MB-231, and HEK-293 cells determined by catalytic detection.

(Figure 4b and Table S1). The copy number of miRNA-21 per pg total RNA in MCF-7 cells determined using our method is consistent with the results obtained from duplex-specific nuclease-assisted detection[13] or qRT-PCR.[31] It is noteworthy that the miRNA-21 target in total RNA could not be detected non-catalytically (Figure 4a), revealing that the catalytic detection is well suited for accurate sensing of nucleic acid targets at relatively low concentration ranges.

Based on the above results, we applied the GNP-QD nanoassembly for in situ detection and imaging of miRNA-21 in live cancer cells. To facilitate uptake of GNP-QD and fuel DNA by the cells, the probe was complexed with Lipofectamine-2000 and then incubated with the cells. Efficient delivery of fuel DNA into cells was achieved, as revealed by confocal microscopy, and the majority of fuel DNA remained intact in cells after 6 hours incubation (Figure S9). As shown in Figure 5a, strong QD PL signals were detected in HeLa, MCF-7, and MDA-MB-231 cells, but not HEK-293 cells, that were incubated with GNP-QD and fuel DNA for 6 hours. In contrast, all of the types of cells incubated with GNP-QD without F exhibited marginal PL signals, which failed to distinguish cancer cells from control cells (Figure 5a). The PL enhancement factors (catalytic vs. non-catalytic) for HeLa, MCF-7, and MDA-MB-231 cells were determined to be 11.5, 9.7, and 12.7, respectively (Figure 5b). These results suggest that catalytic disassembly of GNP-QD could proceed in live cells and be used for high-sensitive imaging of low-abundance nucleic acid biomarkers that are difficult to tackle using conventional probes.

Taken together, we have developed a class of nanoparticle assembly-based probe for accurate sensing of low-abundance miRNA molecules in vitro and in live cells. High sensitivity is achieved through catalytic disassembly of QDs with GNPs to amplify QD PL signals. The LOD of catalytic detection is three orders of magnitude lower than non-catalytic detection, which enables facile and reliable differentiation between cancer cells and normal cells in vitro and in situ. It opens up new opportunities for monitoring low-abundance nucleic acid molecules in live cells, which provides a valuable means for fundamental research and clinical diagnostics.

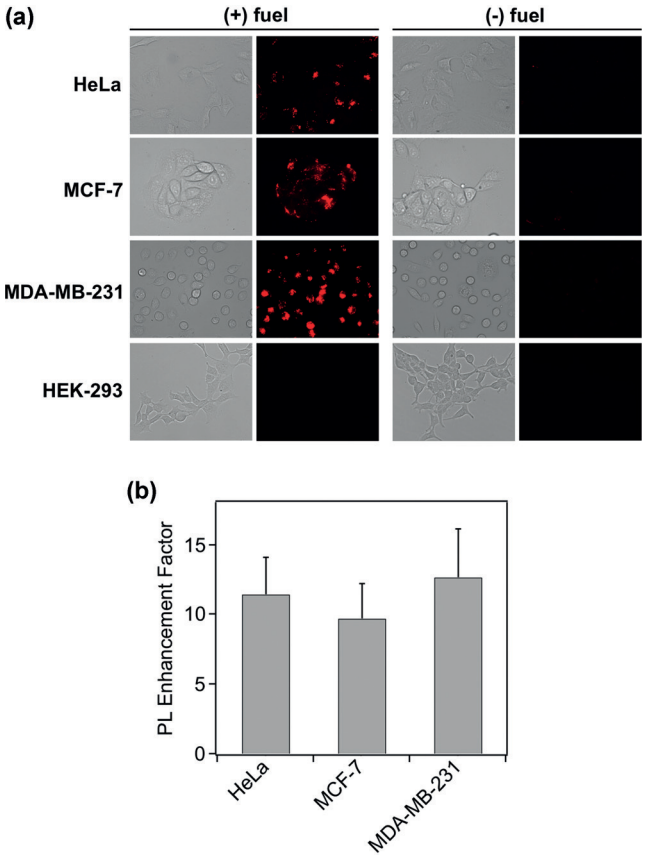

Figure 5. Live-cell imaging of miRNA-21 in HeLa, MCF-7, MDA-MB-231, and HEK-293 cells. a) Fluorescence microscopy images of HeLa, MCF-7, MDA-MB-231, and HEK-293 cells treated with GNP-QDs nanoassembly/fuel DNA (left panel) and GNP-QDs nanoassembly only (right panel). b) PL enhancement factor for catalytic vs. non-catalytic imaging.

Acknowledgements

This work was supported in part by the NSFC (21175147, 91313302, 21475093, 21522506), the National High-Tech R&D Program (2014AA020518), 1000-Young Talents Plan, PAPD, and startup funds from Soochow University.

Keywords: catalysis · gold nanoparticles · microRNAs · molecular imaging · quantum dots

How to cite: *Angew. Chem. Int. Ed.* **2016**, *55*, 3073–3076
Angew. Chem. **2016**, *128*, 3125–3128

[1] L. He, G. J. Hannon, *Nat. Rev. Genet.* **2004**, *5*, 522.
[2] V. Ambros, *Nature* **2004**, *431*, 350.
[3] D. P. Bartel, *Cell* **2004**, *116*, 281.
[4] C. M. Croce, *Nat. Rev. Genet.* **2009**, *10*, 704.
[5] L. He, J. M. Thomson, M. T. Hemann, E. Hernando-Monge, D. Mu, S. Goodson, S. Powers, C. Cordon-Cardo, S. W. Lowe, G. J. Hannon, S. M. Hammond, *Nature* **2005**, *435*, 828.
[6] W. Roa, B. Brunet, L. Guo, J. Amanie, A. Fairchild, Z. Gabos, T. Nijjar, R. Scrimger, D. Yee, J. Xing, *Clin. Invest. Med.* **2010**, *33*, e124.
[7] C. L. Bartels, G. J. Tsongalis, *Clin. Chem.* **2009**, *55*, 623.
[8] S. Tyagi, F. R. Kramer, *Nat. Biotechnol.* **1996**, *14*, 303.
[9] B. Dubertret, M. Calame, A. J. Libchaber, *Nat. Biotechnol.* **2001**, *19*, 365.
[10] P. Zhang, T. Beck, W. Tan, *Angew. Chem. Int. Ed.* **2001**, *40*, 402; *Angew. Chem.* **2001**, *113*, 416.
[11] B.-C. Yin, Y.-Q. Liu, B.-C. Ye, *J. Am. Chem. Soc.* **2012**, *134*, 5064.
[12] H. Jia, Z. Li, C. Liu, Y. Cheng, *Angew. Chem. Int. Ed.* **2010**, *49*, 5498; *Angew. Chem.* **2010**, *122*, 5630.
[13] F. Degliangeli, P. Kshirsagar, V. Brunetti, P. P. Pompa, R. Fiammengo, *J. Am. Chem. Soc.* **2014**, *136*, 2264.
[14] A. F. Jou, C.-H. Lu, Y.-C. Ou, S.-S. Wang, S.-L. Hsu, I. Willner, J. A. Ho, *Chem. Sci.* **2015**, *6*, 659.
[15] R. Deng, L. Tang, Q. Tian, Y. Wang, L. Lin, J. Li, *Angew. Chem. Int. Ed.* **2014**, *53*, 2389; *Angew. Chem.* **2014**, *126*, 2421.
[16] X. Michalet, F. F. Pinaud, L. A. Bentolila, J. M. Tsay, S. Doose, J. J. Li, G. Sundaresan, A. M. Wu, S. S. Gambhir, S. Weiss, *Science* **2005**, *307*, 538.
[17] I. L. Medintz, H. T. Uyeda, E. R. Goldman, H. Mattoussi, *Nat. Mater.* **2005**, *4*, 435.
[18] U. Resch-Genger, M. Grabolle, S. Cavaliere-Jaricot, R. Nitschke, T. Nann, *Nat. Methods* **2008**, *5*, 763.
[19] M. Bruchez, Jr., M. Moronne, P. Gin, S. Weiss, A. P. Alivisatos, *Science* **1998**, *281*, 2013.
[20] W. C. W. Chan, S. Nie, *Science* **1998**, *281*, 2016.
[21] X. Gao, Y. Cui, R. M. Levenson, L. W. Chung, S. Nie, *Nat. Biotechnol.* **2004**, *22*, 969.
[22] H. S. Choi, W. Liu, F. Liu, K. Nasr, P. Misra, M. G. Bawendi, J. V. Frangioni, *Nat. Nanotechnol.* **2010**, *5*, 42.
[23] N. Ma, E. H. Sargent, S. O. Kelley, *Nat. Nanotechnol.* **2009**, *4*, 121.
[24] N. L. Rosi, D. A. Giljohann, C. S. Thaxton, A. K. Lytton-Jean, M. S. Han, C. A. Mirkin, *Science* **2006**, *312*, 1027.
[25] X. Zhang, M. R. Servos, J. Liu, *J. Am. Chem. Soc.* **2012**, *134*, 7266.
[26] S. Park, K. A. Brown, K. Hamad-Schifferli, *Nano Lett.* **2004**, *4*, 1925.
[27] X. He, Z. Li, M. Chen, N. Ma, *Angew. Chem. Int. Ed.* **2014**, *53*, 14447; *Angew. Chem.* **2014**, *126*, 14675.
[28] D. Y. Zhang, A. J. Turberfield, B. Yurke, E. Winfree, *Science* **2007**, *318*, 1121.
[29] S. Zhu, H. Wu, F. Wu, D. Nie, S. Sheng, Y. Y. Mo, *Cell Res.* **2008**, *18*, 350.
[30] S. Ali, K. Almhanna, W. Chen, P. A. Philip, F. H. Sarkar, *Am. J. Transl. Res.* **2011**, *3*, 28.
[31] H.-M. Chan, L.-S. Chan, R. N. Wong, H.-W. Li, *Anal. Chem.* **2010**, *82*, 6911.

Received: October 17, 2015
Revised: November 26, 2015
Published online: December 22, 2015

